*Physics*

*Electricity & Magnetism fields*

Okayama University *Year* 1999

# Effect of continuity of potential on accuracy in magnetic field analysis using nonconforming mesh

Kazuhiro Muramatsu
Okayama University

Yasuhiro Yokoyama
Okayama University

Norio Takahashi
Okayama University

Andrew Nafalski
University of South Australia

Ozdemir Gol
University of South Australia

# Effect of Continuity of Potential on Accuracy in Magnetic Field Analysis Using Nonconforming Mesh

Kazuhiro Muramatsu, *Member, IEEE*, Yasuhiro Yokoyama, Norio Takahashi, *Fellow, IEEE*, Andrew Nafalski, *Senior Member, IEEE*, and Özdemir Göl

***Abstract*—Methods of analyzing magnetic fields in rotating machines using nonconforming meshes, in which only an interpolation technique is applied, are investigated. The effect of the continuity of potentials at nonconforming surfaces on accuracy is examined. It is shown that although the flux distribution is not affected by the discontinuity of the potential, the force and torque are fairly affected by the discontinuity. Therefore, it is shown that a continuous method, or a discontinuous method using a fine mesh should be used especially in force and torque calculation. An analysis of an induction motor is also carried out using a nonconforming mesh.**

***Index Terms*—Electromagnetic analysis, force calculation, mesh generation, rotating machines.**

## I. INTRODUCTION

IN THE ANALYSES of magnetic fields in rotating machines, if the meshes of the rotor and the stator can be generated separately, the problem of mesh generation is simplified. Moreover, the rotor should be able to rotate freely without being restricted by the positions of the nodes at the surfaces of the rotor and stator meshes, to be of practical use. The use of nonconforming meshes [1], in which the positions of adjacent nodes at nonconforming surfaces do not coincide with each other, satisfies the above requirements. Although nonconforming techniques [1], [2] with Lagrangian multipliers have already been developed for the rotating machine, the application of methods [3]–[6] using only an interpolation technique of the potential is also attractive because they are very simple and the matrices do not become ill-conditioned [4].

In this paper, the methods for applying two interpolation techniques with continuous and discontinuous [6] potential distributions at the nonconforming surfaces are described. Then, these methods are compared with each other from the viewpoints of the accuracy of flux distribution and electromagnetic force. To investigate the effectiveness of the nonconforming mesh, an analysis of torque of an induction motor is also accomplished.

Manuscript received October 25, 1999.

K. Muramatsu, Y. Yokoyama, and N. Takahashi are with the Department of Electrical and Electronic Engineering, Okayama University 3-1-1, Tsushima, Okayama 700-8530, Japan (e-mail: {muramatu; norio; yokoyama}@eplab.elec.okayama-u.ac.jp).

A. Nafalski and Ö. Göl are with the Division of Information Technology, Engineering and the Environment, University of South Australia, Mawson Lakes, Adelaide, South Australia 5095, Australia (e-mail: {nafalski; ozdemir.gol}@unisa.edu.au).

Publisher Item Identifier S 0018-9464(00)05655-7.

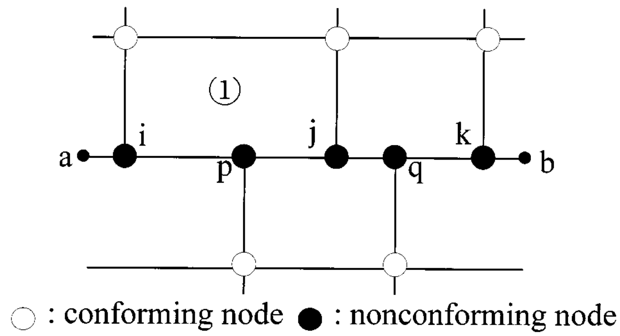


Fig. 1. Mesh with nonconforming nodes.

## II. METHOD OF ANALYSIS

### A. Nonconforming Mesh

A 2-D example of a nonconforming mesh using first-order rectangular elements is shown in Fig. 1. The black circles denote nonconforming nodes. The location of the nodes do not coincide with each other between adjacent elements at the nonconforming surface $a$–$b$. When the nonconforming technique is applied in the gap between the rotor and the stator in rotating machines, the meshes can be generated separately and the rotor can be rotated freely without being restricted by the positions of the nodes. When the analysis using this mesh is carried out, the potentials at the nonconforming surface have to be interpolated in terms of those on the opposite side in order to have a relationship between each other. In the next section, methods of interpolation with the discontinuous and continuous potential distributions are described.

### B. Discontinuous Method

In this method, the potentials of the nonconforming nodes on one side, where the mesh density is larger, are interpolated by those on the opposite side. For example, the potentials at the nodes $p$, $q$ are linearly interpolated by those at the nodes $i$, $j$ and $k$ in Fig. 1. In this case, the potentials on the line $a$–$b$ become discontinuous with each other as shown in Fig. 2, because the potential in each element changes individually and linearly. We call this method the “discontinuous method.” The software in this method can be simple but the effect of the discontinuity of potential on accuracy should be examined.

### C. Continuous Method

In order to modify the discontinuous potential distribution to the continuous one, the temporary mesh, which is generated by

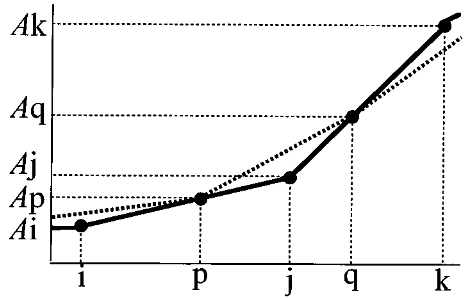


Fig. 2. Potential distributions along lin $a$–$b$.

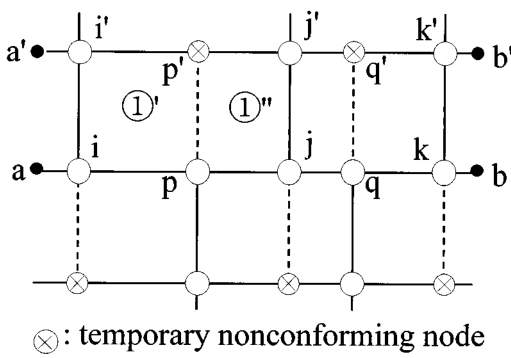


Fig. 3. Modified temporary mesh.

subdividing the elements including the nonconforming nodes on the edges, is used [5]. For example, the original element ① in Fig. 1 is subdivided into the temporary elements ①′ and ①″ as shown in Fig. 3. Then, the nonconforming nodes on the line $a$–$b$ become the conforming ones and, for example, the temporary nonconforming node $p'$ is newly added on the line $a'$–$b'$. The temporary nonconforming node $p'$ is linearly interpolated by the adjacent conforming nodes $i'$ and $j'$, and the potentials on the line $i'$–$j'$ become continuous because the potentials are interpolated by only the potentials of nodes $i'$ and $j'$. As a result, the potentials on the line $a'$–$b'$ become continuous as shown in Fig. 4. We call this method the "continuous method." In this method, the potentials can be continuous in the whole region but the software becomes complex due to the reconstruction of the mesh.

## III. Effect of Continuity of Potential on Accuracy

### *A. Analyzed Model and Conditions*

A 2-D simple model is shown in Fig. 5. In this model, the flux is produced by the magnet and an electromagnetic force is generated between the magnet and the pole piece. The relative position, $D$, between the magnet and the pole piece is changed from 0–5 mm. The magnetization of the magnet and the relative permeability of the pole piece are assumed to be equal to 1 T and 1000 respectively. The eddy currents in the magnet and the pole piece are neglected.

The whole meshed region is subdivided into coarse and fine first-order rectangular elements. Fig. 6 shows the coarse mesh at $D = 4.75$ mm. The meshes on the magnet and pole piece sides are generated separately and the meshes are put together at the

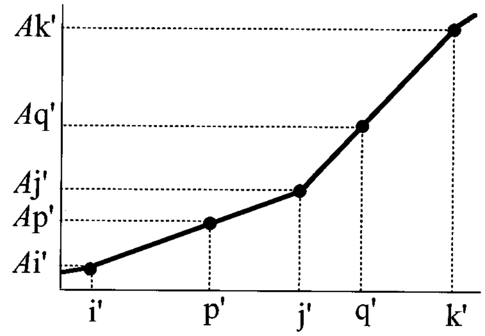


Fig. 4. Potential distributions along line $a'$–$b'$.

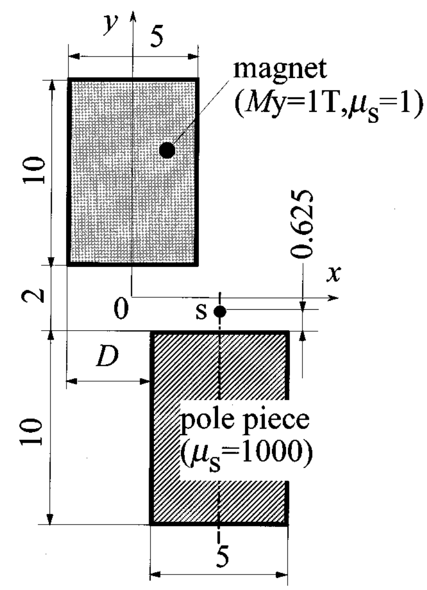


Fig. 5. Analyzed model.

arbitrary position $D$. The meshes are divided uniformly in the $x$-direction and the mesh sizes in this direction for the coarse and fine meshes are 1 mm and 0.5 mm respectively. Therefore, the coarse and fine meshes become the ordinary conforming meshes when $D$ is a multiple of 1 mm and 0.5 mm.

The periodic boundary conditions are imposed on boundaries $b$–$c$–$d$–$e$ and $a$–$h$–$g$–$f$ and the Dirichlet boundary conditions are imposed on the boundaries $a$–$b$ and $e$–$f$.

### *B. Results and Discussion*

Fig. 7 shows the flux distribution at $D = 4.75$ mm obtained from the discontinuous method with the coarse mesh. Fig. 8 shows the change of the $y$-component of flux density, $B_y$, at the point s, shown in Fig. 5, with $D$ when the coarse mesh is used. The symbols □ and ◊ and in Figs. 8 and 9 denote that the results are obtained from the ordinary conforming meshes. The results obtained from the discontinuous and continuous methods in Fig. 8 are both reasonable, because they change smoothly even if the meshes become of the nonconforming type. Moreover, the error due to the discontinuity of potential may be neglected for the calculation of flux distribution, because the two cases are in good agreement with each other.

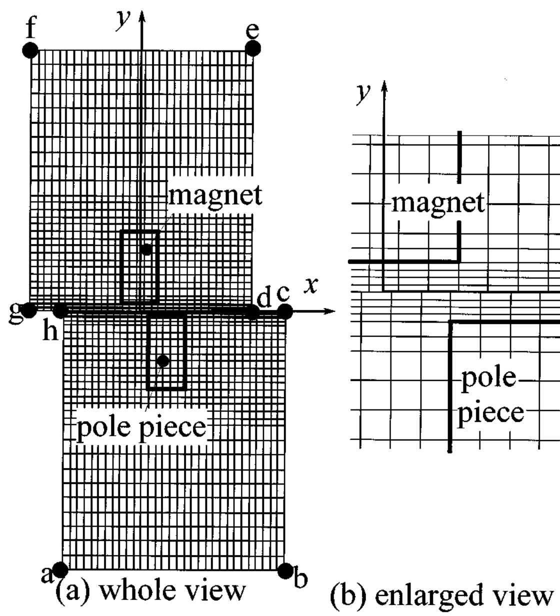


Fig. 6. Mesh (coarse mesh, $D = 4.75$).

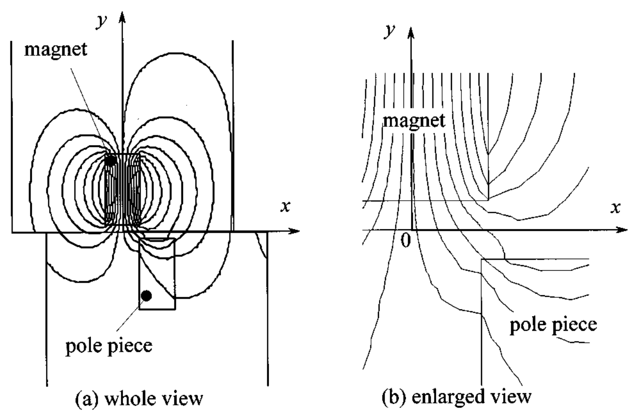


Fig. 7. Flux distribution (discontinuous method, coarse mesh) $D = 4.75$.

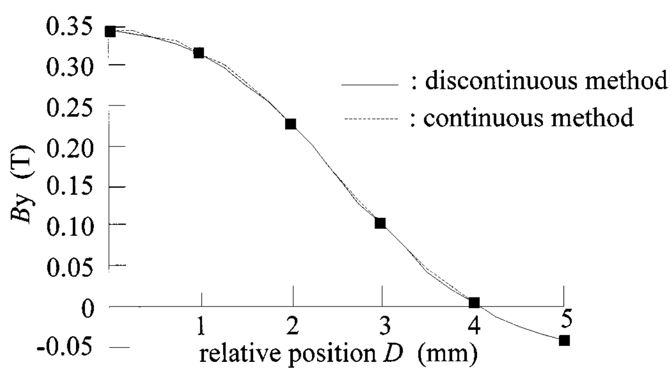


Fig. 8. Change of flux density (coarse mesh).

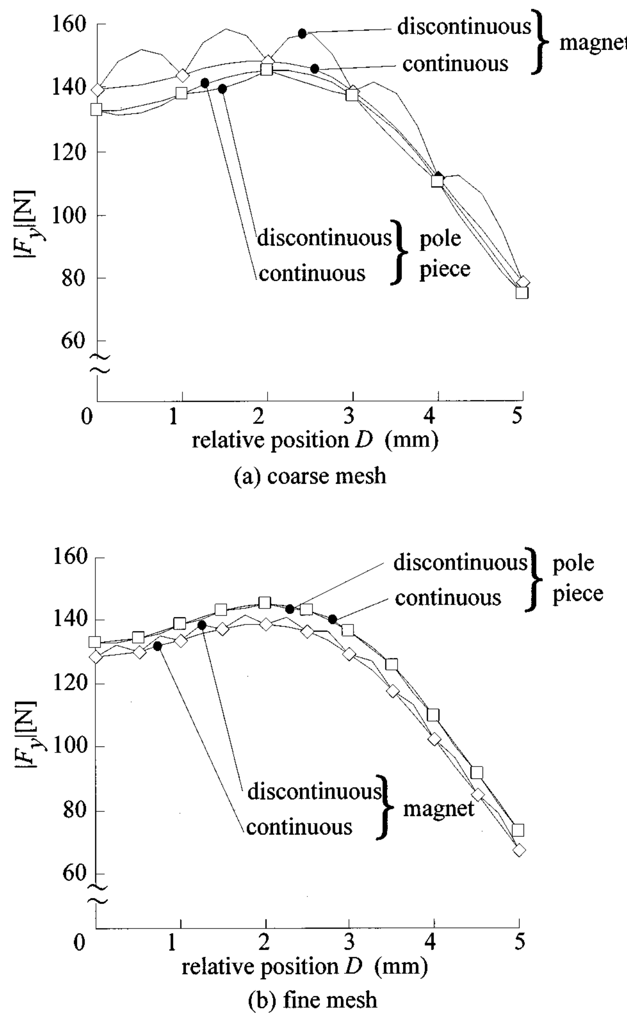


Fig. 9. Change of electromagnetic force.

Fig. 9 shows the changes of the $y$-component of the electromagnetic force, $|F_y|$, of the magnet and the pole piece with $D$. The electromagnetic force is calculated by the nodal force method [7]. Although the electromagnetic force should change smoothly with $D$ as for results by the continuous method, the results obtained from the discontinuous method have spurious oscillations. Therefore, the effect of the discontinuity of potential on the electromagnetic force cannot be neglected, because higher accuracy is required for force calculation. Fig. 9(b) shows that the spurious oscillation in the discontinuous method can be reduced if the fine mesh is used. Therefore, in order to evaluate the electromagnetic force using the nonconforming mesh, the continuous method, or the discontinuous method with fine mesh, should be used.

## IV. Application

A nonconforming technique is applied to a 2D magnetic field analysis in an induction motor in order to investigate its effectiveness .

### A. Model

Fig. 10 shows the model of an induction motor without skew. The motor is one of the verification models proposed by the IEEJ. The detailed data of this motor is shown in Table I. The rotor and stator cores are made of the silicon steel 50A1300 and the nonlineality is taken into account. The conductivity of the aluminum rotor bar is assumed to be $1.02 \times 10^7$ S/m by revising

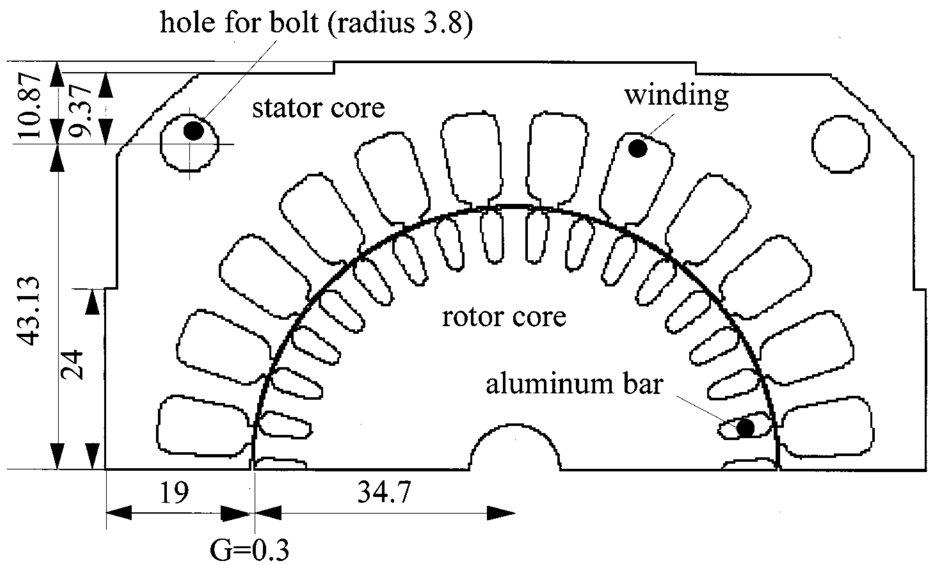


Fig. 10. Induction motor (thickness: 42 mm).

TABLE I
DETAILS OF INDUCTION MOTOR

| | |
|---|---|
| Rated line voltage | 100V, 50Hz |
| Number of poles | 4 poles |
| Connection | star |
| Air-gap length | 0.3mm |
| Gross core length | 42mm |
| Number of turns per slot | 66 |
| Resistance per phase | 2.92Ω |
| Conductivity of bar | $2.1 \times 10^{7}$ S/m |

the conductivity to 2-D analysis. Only 1/2 of the whole region is analyzed due to symmetry.

### B. Meshes and Analyzed Condition

Fig. 11 shows the mesh with the first order quadrilateral elements. The nonconforming technique is applied in the gap between the rotor and the stator. The mesh is made fine enough to neglect the effect of the discontinuity of the potential. The total number of elements and nodes are 23 778 and 24 790, respectively. The discontinuous method is applied. The steady state is obtained using the step-by-step method. The time interval $\Delta t$ is chosen so that the rotor rotates at 0.88 deg. during $\Delta t$. The periodic boundary condition is used.

### C. Results and Discussion

Fig. 12 shows the waveforms of the torque at steady state at 1125 rpm. As the time interval $\Delta t$ can be chosen to be small enough without being restricted by the positions of the nodes by using the nonconforming technique, the high frequency phenomena can be also evaluated.

The current and the torque obtained from the calculation are compared with measurements and are shown in Fig. 13. The results show that the calculated and the measured values are in good agreement.

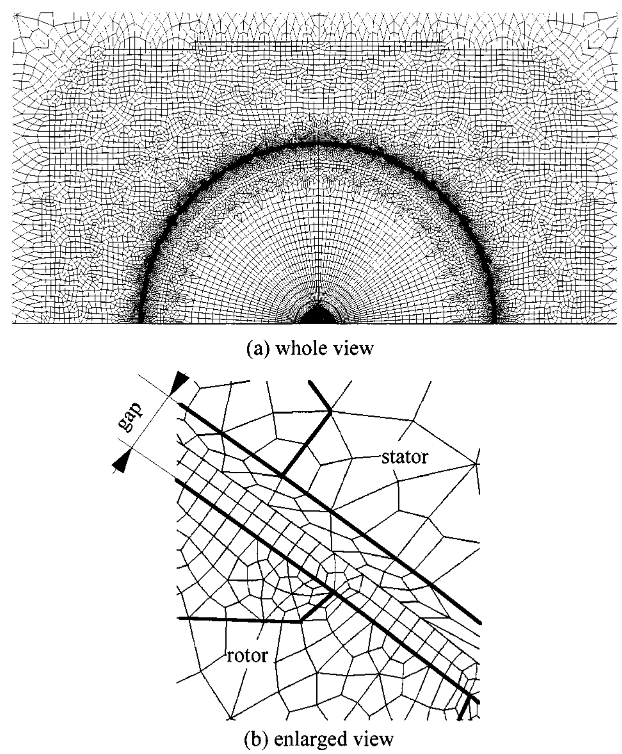


Fig. 11. Mesh of induction motor.

## V. CONCLUSIONS

The effect of the continuity of potential on accuracy is investigated in the magnetic field analysis using the nonconforming mesh. The nonconforming technique is also applied to the induction motor.

The results obtained can be summarized as follows:

1) The interpolation techniques with continuous and discontinuous potential distributions at the nonconforming surfaces of rotating machines are described.

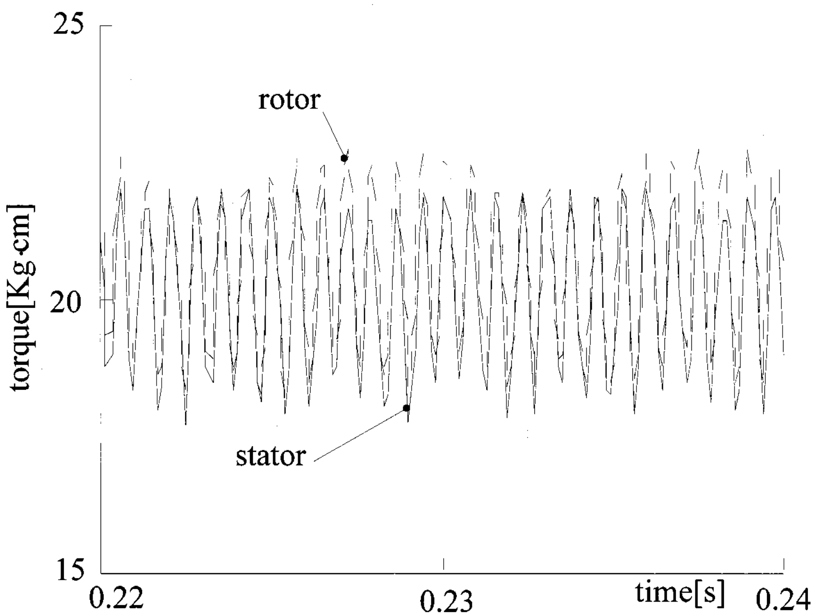


Fig. 12. Wafeform of torque [1125 rpm ($s = 0.25$)].

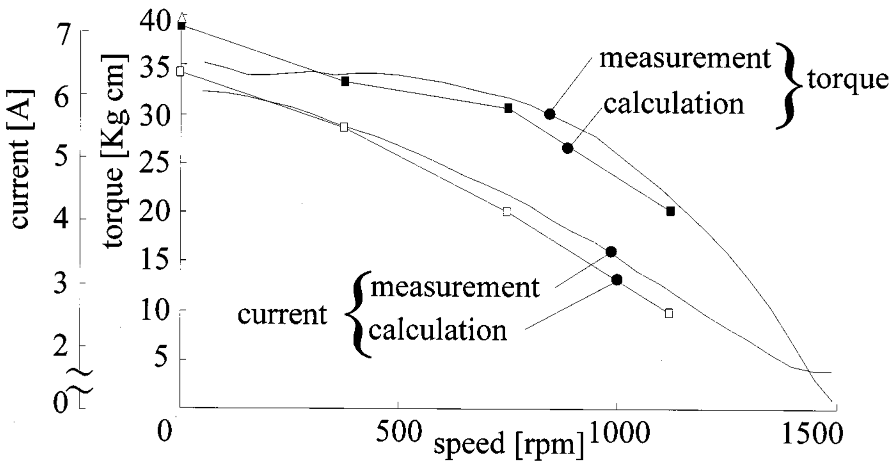


Fig. 13. Comparison between calculation and measurement.

2) The flux distribution is not affected by the discontinuity of the potential.
3) The force is affected by the discontinuity of the potential. Therefore, the continuous method, or the discontinuous method using a finer mesh compared with the ordinary finite element method, should be used for force calculation.
4) The effectiveness of the method using the nonconforming mesh is shown in the analysis of the induction motor.

## ACKNOWLEDGMENT

The authors would like to thank the committee of IEEJ (chairman: Dr. S. Sakabe) who provided the model and the measured data of the induction motor in this paper.

## REFERENCES

[1] D. Rodger, H. C. Lai, and P. J. Leonard, “Coupled elements for problems involving movement,” *IEEE Trans. Magn.*, vol. 26, no. 2, pp. 548–550, 1990.
[2] Y. Marechal, G. Meunier, J. L. Coulomb, and H. Magnin, “A general purpose tool for restoring inter-element continuity,” *IEEE Trans. Magn.*, vol. 28, no. 2, pp. 1728–1731, 1992.
[3] A. Raizer, S. R. H. Hoole, G. Meunier, and J. L. Coulomb, “p- and h-type adaptive mesh generation,” *J. Appl. Phys.*, vol. 67, pp. 5803–5805, 1990.
[4] K. Muramatsu, T. Nakata, N. Takahashi, and K. Fujiwara, “Investigation of effectiveness of 3-D nonconforming mesh,” *IEEE Trans. Magn.*, vol. 27, no. 6, pp. 5211–5213, 1991.
[5] ——, “3-D adaptive mesh refinement using nonconforming elements,” *IEEE Trans. Magn.*, vol. 29, no. 2, pp. 1479–1482, 1993.
[6] H. Kometani, S. Sakabe, and A. Kameari, “3-D analysis of induction motor with skewed slots using regular coupling mesh,” in *The Proceedings of the Compumag’99*, Sapporo, 1999, no. PA4-8.
[7] A. Kameari, “Local force calculation in 3-D FEM with edge elements,” *Int. J. Appl. Electromagn. in Materials*, vol. 3, pp. 231–240, 1993.